

Frequency dependence of pyroelectric current in poly(vinylidene fluoride) heat sinked at various temperatures

L. F. Hu, K. Takahashi, R. E. Salomon, and M. M. Labes

Citation: *Journal of Applied Physics* **50**, 2910 (1979); doi: 10.1063/1.326210

View online: <http://dx.doi.org/10.1063/1.326210>

View Table of Contents: <http://scitation.aip.org/content/aip/journal/jap/50/4?ver=pdfcov>

Published by the AIP Publishing

Articles you may be interested in

[Equilibrium polarization and piezoelectric and pyroelectric coefficients in poly\(vinylidene fluoride\)](#)

J. Appl. Phys. **57**, 902 (1985); 10.1063/1.334690

[The pressure and temperature dependence of piezoelectric and pyroelectric response of poled unoriented phase I poly\(vinylidene fluoride\)](#)

J. Appl. Phys. **53**, 6557 (1982); 10.1063/1.330083

[The poling field and draw dependence of the piezoelectric and pyroelectric response of pressure-quenched, phase I poly\(vinylidene fluoride\) films](#)

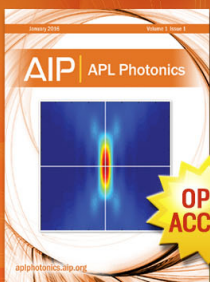
J. Appl. Phys. **52**, 5983 (1981); 10.1063/1.329817

[Plasma poling of poly\(vinylidene fluoride\): Piezo- and pyroelectric response](#)

J. Appl. Phys. **51**, 1676 (1980); 10.1063/1.327775

[Some aspects of piezoelectricity and pyroelectricity in uniaxially stretched poly\(vinylidene fluoride\)](#)

J. Appl. Phys. **48**, 513 (1977); 10.1063/1.323695



Launching in 2016!

The future of applied photonics research is here

AIP | APL
Photonics

Frequency dependence of pyroelectric current in poly(vinylidene fluoride) heat sinked at various temperatures

L. F. Hu, K. Takahashi, R. E. Salomon, and M. M. Labes^{a)}

Department of Chemistry, Temple University, Philadelphia, Pennsylvania 19122

(Received 6 September 1978; accepted for publication 24 October 1978)

The frequency and temperature dependences of pyroelectric activity in poly(vinylidene fluoride) have been studied from 10 to 369°K using mechanically chopped and steady-state radiation. From these data, thermal diffusivity and a parameter indicating the polarization inhomogeneity can be deduced and compared with a mathematical model.

PACS numbers: 77.70. + a, 85.50.Ly, 66.70. + f, 77.55. + f

I. INTRODUCTION

In the utilization of poly(vinylidene fluoride), PVF₂, as an optical-radiation detector, the frequency response characteristics have been mathematically modeled by considering the interaction of two factors: (a) the inhomogeneity (or homogeneity) of the sample polarization as a consequence of the poling conditions, and (b) the thermal diffusivity of the pyroelectric material.¹⁻⁴ In this work, the frequency response to a pulsed heat input of a heat-sinked PVF₂ film is examined. The temperature of the heat sink is varied from 369 to 10°K. Pyroelectric coefficients and thermal diffusivity are determined for PVF₂ in this temperature range. These experiments allow one to measure thermal diffusivity over a sufficient temperature range to check the validity of the mathematical model proposed by Peterson *et al.*¹ to ascertain the inhomogeneity of polarization, and to determine the temperature dependence of the pyroelectric coefficient well above and below the glass transition temperature of this semicrystalline polymer.

THEORY

A general description and solution for various boundary conditions of a pyroelectric detector have been described elsewhere in detail.¹ In this paper, the specific case considered is one in which one side of a PVF₂ film is kept at a fixed temperature with a heat sink, while the other surface is exposed to a chopped optical beam. Assuming that the input heat of the chopped optical beam is absorbed on the front surface without any loss and heat flow is only in the x direction normal to the surface, one can express the current density resulting from changing the temperature of the pyroelectric film as¹

$$J(t) = \frac{1}{L} \int_0^L dx \frac{dP}{dT} \frac{dT(x,t)}{dt}, \quad (1)$$

where L is the thickness of the pyroelectric film, T is the temperature, t is the time, and dP/dT is the pyroelectric coefficient. For convenience, the functional relationship to express the nonuniformity of the pyroelectric coefficient throughout the film used in this calculation is

$$\frac{dP}{dT} = P_0 \exp\left(-\frac{\xi x}{L}\right), \quad (2)$$

where P_0 is the surface pyroelectric coefficient and ξ is the parameter of nonuniformity.¹ One-dimensional heat flow in the film gives

$$\frac{dT}{dt} = \alpha \frac{d^2 T}{dx^2}, \quad (3)$$

where α is the thermal diffusivity. The term α is defined as

$$\alpha = \frac{k}{C_v}, \quad (4)$$

where k is the thermal conductivity and C_v is the heat capacity per unit volume at constant pressure. Equation (3) is solved using the following boundary conditions: a perfect heat sink keeps one end of the film at a constant temperature,

$$T(x = L, t) = T_0; \quad (5)$$

heat is supplied in some specified manner to the exposed face at $x = 0$, expressed by

$$Q = -k \frac{dT}{dx}, \quad (6)$$

where Q is the heat input. The steady-state current response to a sinusoidal heat input at frequency w_0 is given in Ref. 1 as

$$|J(w_0)| = \left(\frac{P_0 Q_0}{LC_v}\right) |\bar{\gamma}(iw_0)|, \quad (7)$$

where Q_0 is the incident heat. The complex response function $\bar{\gamma}(iw)$ to the heat input is

$$\begin{aligned} \bar{\gamma}(iw) = & \mu [\exp(-2W_p) - 1] + [1 + \exp(-2W_p)] \\ & - 2 \exp(-\xi - W_p) \\ & \times \{[1 + \exp(-2W_p)](1 - \mu^2)\}^{-1}, \end{aligned} \quad (8)$$

where $W_p = (iw/\alpha)^{1/2} L$ and $\mu = \xi/W_p$. The magnitude of the current density $|J(W_0)|$ in Eq. (7) is obtained by calculating $[\bar{\gamma}(iW_0)\bar{\gamma}^*(iW_0)]^{1/2}$.

EXPERIMENTAL

Both sides of biaxially stretched 6- μ PVF₂ films, obtained from Kureha Chemical Corporation, were vacuum deposited with nichrome electrodes. The thickness and area

^{a)}Work was supported by the U.S. Army Research Office under Grant No. DAAG29-76-G-0040.

TABLE I. Maximum pyroelectric currents under various poling conditions as a function of temperature.

Sample ^a	Poling conditions ^b		Pyroelectric coeff. at 308 °K ^c (nC cm ⁻² K ⁻¹)	Pyroelectric response (μV)							
	E_p (MV cm ⁻¹)	t_p (min)		20 °K	50 °K	100 °K	150 °K	200 °K	233 °K	250 °K	290 °K ^d
20 +	1	60	0.92	5.2	5.6	5.1	4.9	4.1	...	4.5	5.3
20 -	1	60	1.10	2.9	2.8	2.3	1.9	1.8	1.8	1.9	2.2
21 +	1	60	1.37	5.3	4.2	4.1	4.6	4.6	4.8	5.0	6.1
21 -	1	60	1.48	4.0	4.3	4.0	3.6	3.4	3.4	3.6	4.3
25 +	2	30	2.80	4.4	4.5	3.9	3.5	3.2	3.2	3.4	4.0
25 -	2	30	2.60	2.9	3.0	2.7	2.6	2.5	2.3	2.5	3.1
26 +	2	30	2.60	6.5	6.6	6.2	5.5	5.2	5.4	...	6.9
26 -	2	30	2.77	5.4	5.5	5.0	4.5	4.1	4.0	4.0	4.6
75 +	1	60	1.15	4.8	5.1	4.6	4.2	3.9	4.0	4.2	5.1
1 +	1	30	26
1 -	1	30	12
2 +	1	60	1.26	24
2 -	1	60	1.30	17
3 +	2	30	2.56	20
3 -	2	10	2.65	13
4 +	3	5	2.96	26
4 -	3	5	2.82	25

^aSamples designated by the same number indicate pairs which were prepared identically. The notation + and - indicates irradiation on the positively poled side or negatively poled side, respectively.

^b E_p and t_p are poling field and time, respectively.

^cMeasured by the conventional method.

^dIncident light intensity used in irradiating samples 1-4 was much larger than all other samples, and hence absolute currents are also larger.

of the electrodes were 150 Å and 1.3 cm², respectively. Electrical leads were attached with conducting epoxy adhesive (Acme Chemical, No. 3021). The samples were poled at 60 °C with fields of 1, 2, or 3 MV cm⁻¹. For the first heating cycle, the poled films were heated at 10 °C min⁻¹ from the poling temperature of 60 up to 80 °C and kept at 80 °C for 10 min in the short-circuit configuration. The samples were then cooled to room temperature. During a second heating cycle, the samples were heated at 2 °C min⁻¹ and pyroelectric currents were measured. Pyroelectric coefficients were calculated at a temperature of 35 °C. A detailed description of this measurement and the subsequent calculation of the pyroelectric coefficient are reported elsewhere.⁵ For poling of films at fields of more than 2 MV cm⁻¹, a dielectric liquid (Fluorinert FC-77) was used. During poling, the films were dipped in the liquid to prevent short circuits in the film.

The poled films were mounted on two different heat sinks, one for the experiments at room temperature, and the other for experiments at various temperatures ranging from 10 to 369 °K. For the experiments at room temperature, Cry-Con Grease (Air Products and Chemicals) or General Electric No. 7031 adhesive insulating varnish was used to attach the sample to a copper-plate heat sink. The copper plate was mounted in an aluminum box for shielding to prevent extraneous noise. For experiments at various temperatures, the films were glued to the plane of a copper column, which was used as a heat sink, with General Electric No. 7031. The copper column was mounted in a Displex Cryostat (Air Products and Chemicals, Model CSA-202). A chromel-alumel thermocouple was placed in a hole in the copper column with Cry-Con Grease so that the heat-sink temperature could be read out with a millivolt potentiometer or Keithley 160 Digital Multimeter. For both cases, the back nichrome electrode was grounded to the heat sink. The upper nichrome electrode was connected to a lock-in amplifier (PAR

Model 124). A load resistor of 47 kΩ was inserted in parallel with the sample. A tungsten lamp was used as the heat source. The light beam was chopped with a PAR Model 222 chopper to form a square wave. The signal response was measured from a low frequency of 10 Hz to a high frequency of 4500 Hz.

Experiments with the heat sink at various temperatures were carried out in a vacuum since this is a requirement for

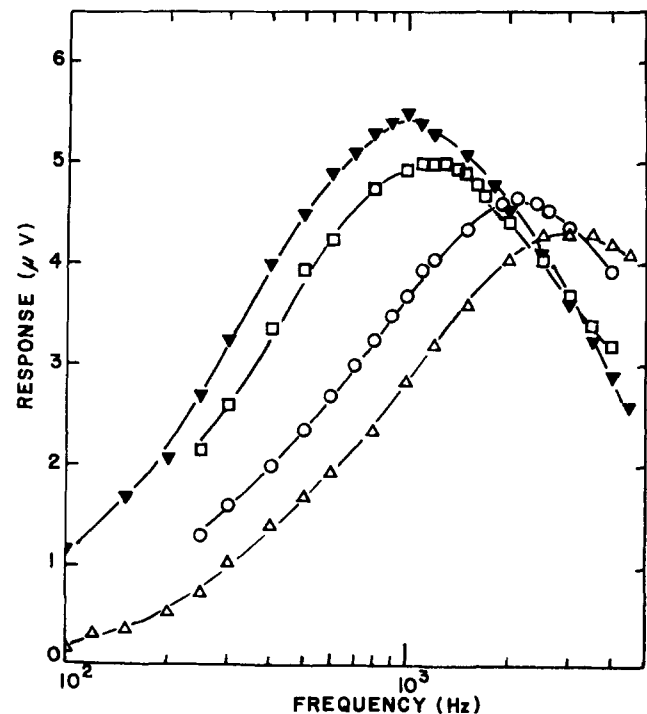


FIG. 1. Pyroelectric response versus log (frequency) at different temperatures for sample 21 + ▴, 290 °K; □, 250 °K; ○, 150 °K; △, 50 °K.

TABLE II. Nonuniformity parameter ξ for various samples as a function of temperature.

Sample	20 °K	50 °K	100 °K	Values of ξ at various temperatures				
				150 °K	200 °K	233 °K	250 °K	290 °K
20	0.6	0.7	0.8	1.0	0.9	...	0.9	0.9
21	0.3	0.0	0.0	0.3	0.3	0.3	0.3	0.3
25	0.4	0.4	0.4	0.3	0.3	0.3	0.3	0.3
26	0.2	0.2	0.2	0.2	0.3	0.3	...	0.4
1	0.8
2	0.3
3	0.4
4	0.0

use of a Displex Cryostat. At 290 °K experiments were conducted in both vacuum and air. Since the results were essentially the same, the thermal conductivity of air could be neglected. To determine the effect of the thickness variation of the heat-absorbing nichrome electrode, a sample in which the electrode thickness of the exposed side was half of that of the typical thickness (150 Å) was prepared. The results in terms of the chopper frequency, the magnitude of the maximum pyroelectric current, and the overall shape of the curve were the same indicating a negligible effect of the absorber thickness, at least in these experimental ranges of heat-sink temperature and chopper frequency.

To check linearity of response (which will be crucial to the subsequent analysis), the incident light was varied by placing screens between the light and the sample and was measured with a thermopile. It was found that the pyroelectric response varied linearly with the incident light of the frequency range used in this experiment.

RESULTS AND DISCUSSION

Typical curves of the pyroelectric current versus the chopper frequency are shown in Fig. 1. The chopper frequency at the maximum pyroelectric current in the curve shifted with the heat-sink temperature. At the lower temperature, the maximum current appeared at the higher frequency. Pairs of samples were examined for a comparison

between the cases for radiation absorbed on the positively and negatively poled side. At any temperature of the heat sink, the positively poled side always has a larger pyroelectric current than the corresponding negatively poled side, as shown in Table I.

The results in Table II show that the distribution of polarization through the film is not uniform. It is generally assumed that dP/dT varies with x as $P_0 \exp(-\xi x/L)$, where x is the distance through the film from the irradiating electrode, L is the thickness of the film, and P_0 is the surface pyroelectric coefficient.¹ When the measurement is made with the negatively poled side exposed to the chopped radiation, dP/dT can be expressed as $P_0 \exp(-\xi) \exp(\xi x/L)$. From the results, it is obvious that the value of ξ should be positive. The theoretical and experimental curves were superimposed, enabling us to find a value for ξ by matching magnitudes of the maximum pyroelectric currents and frequencies.

These ξ values determined for samples measured at low temperatures and at room temperature are listed in Table II. It is apparent that the larger ξ is due to a greater nonuniformity of the polarization. When the poling field is smaller, a greater inhomogeneity of polarization is produced through the film. These results are basically in agreement with the literature results.⁴

According to the theoretical model,¹ W_p is a function of

TABLE III. Temperature dependence of frequency (Hz) at which maximum pyroelectric current is observed.

Sample ^a	20 °K	50 °K	100 °K	Peak frequency (Hz)				
				150 °K	200 °K	233 °K	250 °K	290 °K
20 +	3000	2600	2300	2000	1700	...	1000	900
20 -	3300	2900	2200	1900	1600	1300	1100	1000
21 +	3400	3000	2600	2250	1800	1400	1200	1000
21 -	3200	2700	2300	1800	1500	1300	1000	900
25 +	3500	3100	2300	2000	1700	1300	1300	1000
25 -	3700	3000	2400	1850	1700	1450	1150	1000
26 +	3700	3000	2500	1750	1600	1250	...	1050
26 -	3000	2700	2200	1900	1500	1200	1050	800
75 +	3600	3000	2500	2100	1900	1500	1200	1050
Average								
+	3440	2940	2440	2020	1680	1360	1180	1000
-	3300	2830	2280	1860	1580	1310	1080	930

^aSample notation is the same as described in Table I.

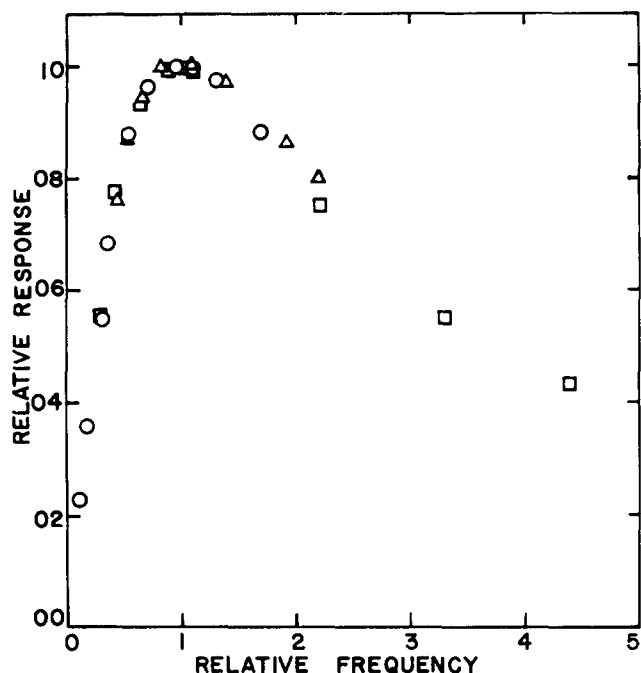


FIG. 2. Relative pyroelectric response versus relative frequency at three different temperatures. \square , 290 °K; \triangle , 150 °K; \circ , 50 °K.

the thermal diffusivity α . Thus, the quantity W_p is temperature dependent and causes the frequency of the maximum pyroelectric current to vary with temperature. To verify this, it is necessary to determine whether the shape of the frequency-dependent pyroelectric current, and hence the ξ value, was affected by changing the temperature. Data obtained at three different temperatures were replotted as shown in Fig. 2. It is apparent that the overall shape of the curves are not

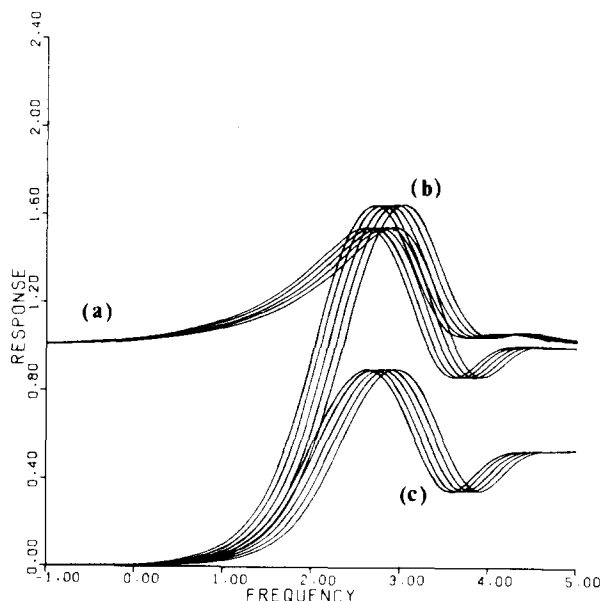


FIG. 3. Pyroelectric response versus log (frequency) using literature thermal diffusivity data. Curve a, $\xi = 0$ (uniform polarization); curve b, $\xi = 0.6$, positively poled side irradiated; and curve c, $\xi = 0.6$, negatively poled side irradiated. The five curves from left to right are for temperatures of 290, 250, 233, 200, and 150 °K, respectively.

affected by varying the temperature, although the original frequency-dependent curves have different frequencies and magnitudes at the maximum pyroelectric current. Also, the values of ξ at low temperatures were not significantly changed as listed in Table II. Therefore, the values of ξ or the distribution of polarization is temperature independent and the shift of the frequency at the peak pyroelectric current is caused by the change of α at a different temperature, that is, the value of the thermal diffusivity k/C_v .

Using available data for thermal diffusivity,⁶ theoretical response curves were plotted at different temperatures as shown in Fig. 3. In each curve a single peak appears at a certain frequency below 10^4 Hz, and the shift of the frequency at the peak is observed at different temperatures. The peak arising for the case of irradiation on the positively poled side appeared at a slightly higher frequency than the one for the reverse case even at low temperatures. This characteristic was observed for all the experimental results shown in Table III.

Experimental values of thermal diffusivity at different temperatures were calculated from the peak frequencies. Using these thermal diffusivity data and available heat capacity data,⁷ the thermal conductivities at different temperatures were calculated. These results are listed in Table IV and thermal conductivities versus temperatures are plotted in Fig. 4. Some slight differences exist between the results obtained and the available literature values. The peak frequency in the theoretical curve is at 600 Hz at room temperature, and does not match precisely with the peak observed experimentally (1000 Hz). These discrepancies are probably due to such differences as molecular-weight distribution in the polymer samples and the differences in the methods of preparation, one set of data being taken on film pressed from a powder and the other on a biaxially stretched film.

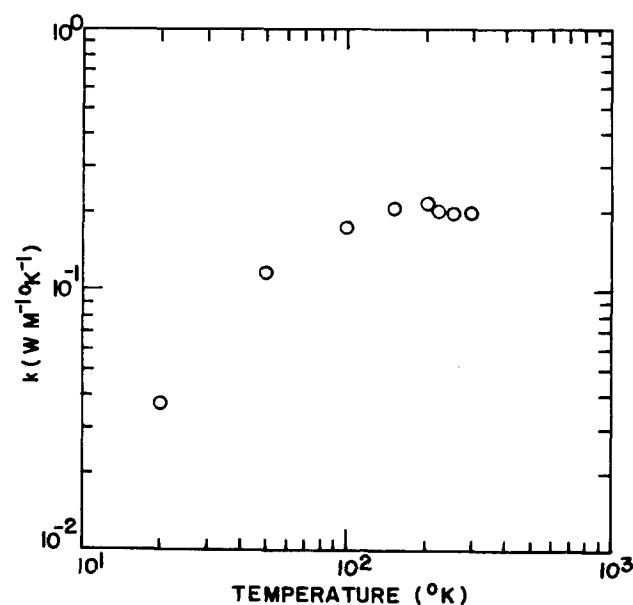


FIG. 4. Log-log plot of thermal conductivity versus temperature.

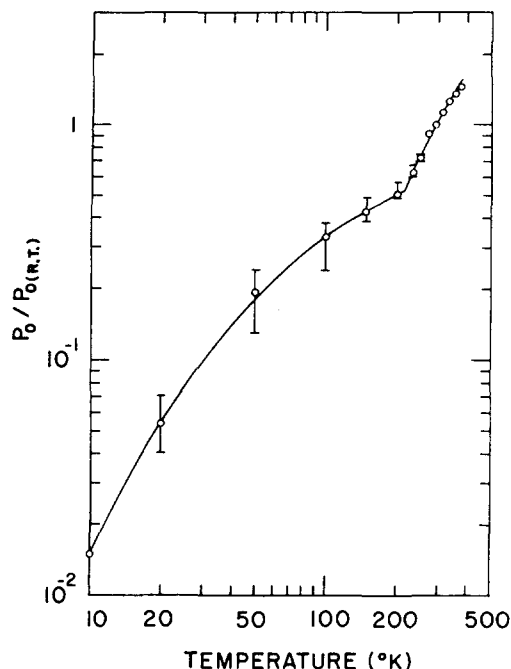


FIG. 5. Log-log plot of normalized pyroelectric coefficient versus temperature.

The thermal conductivity of the film can be treated by a two-phase model in which the conductivity of the amorphous regions is essentially isotropic while that of the crystalline regions is highly anisotropic. The thermal conductivities obtained here are for the direction perpendicular to the crystals with the chain axes parallel to the stretching direction. At temperatures of more than 100 °K, a leveling off of the thermal conductivity was observed. This is probably due to the conductivity via the weak Van der Waals interactions perpendicular to the chains, which is undoubtedly much smaller than through the strong covalent bonds along the chains. Thus, crystallites aligned parallel to the stretching direction contribute more to the thermal conductivity. At temperatures lower than 100 °K, a sharp decrease of the conductivity was observed. As the phonon wavelength becomes greater than the size of the crystallites at these temperatures, the acoustic mismatch at the crystalline or crystalline-amorphous boundaries may give rise to a sharp increase in thermal resistance.

The pyroelectric current J is given by $(P_0 Q_0 / LC_0) | \gamma |$. The quantity of heat Q_0 and the thickness L are constant. The magnitude of the pyroelectric current J is a function of P_0 and C_0 , which are temperature-dependent parameters. Using literature data for C_0 ,⁷ the relative pyroelectric coefficients of a given film at different temperatures can be calculated by taking a ratio. The results are shown in Fig. 5. It can be seen that the relative pyroelectric coefficient increases with increasing temperature. The nature of the temperature dependence changes at ~ 220 °K. Below this temperature, the pyroelectric coefficients are moderately temperature dependent but above this temperature they exhibit a T^2 dependence. The temperature of 220 °K is close to the glass transition temperature of PVF₂.⁸ Probably below the temperature of 220 °K the material becomes stiff with no expansion of volume and the primary coefficient is the main contribution, while above this temperature, the thermal expansion of the film becomes large and the secondary coefficient contributes significantly. The pyroelectric coefficients in the temperature range between 253 to 373 °K are found to exhibit a T^3 dependence using the conventional method of pyroelectric measurements.⁹ The reason for the different temperature dependences of the pyroelectric coefficients in this temperature range may be related to the temperature dependences both of the heat capacity and thermal conductivity. A dilatometric study shows an $\sim T^2$ dependence of thermal expansion of PVF₂ in the temperature range between 243 and 373 °K,¹⁰ offering additional evidence that pyroelectric coefficients in this temperature range are associated with thermal expansion.

CONCLUSIONS

Pyroelectric coefficients for PVF₂ have been measured from 10 to 369 °K. The pyroelectric coefficients are moderately temperature dependent from 10 °K to the glass transition temperature and exhibit a T^2 dependence from the glass transition temperature to 369 °K.

The inhomogeneity introduced by poling is shown to be temperature independent. This strongly suggests that the origin of pyroelectricity in PVF₂ cannot be based on an equilibrium thermodynamic model, such as the Devonshire model of ferroelectrics.¹¹

TABLE IV. Comparison of calculated thermal conductivity and diffusivity with literature values.

Temp. (°K)	Thermal conductivity		Diffusivity	
	Calculated (W m ⁻¹ °K ⁻¹)	Literature (Ref. 7) (W m ⁻¹ °K ⁻¹)	Calculated (× 10 ⁷ m ² sec ⁻¹)	Literature (Ref. 7) (× 10 ⁷ m ² sec ⁻¹)
290	0.200 ^a	0.200	0.92 ^a	0.92
250	0.199	0.196	1.07	1.08
233	0.204	0.193	1.21	1.13
200	0.222	0.187	1.58	1.29
150	0.205	0.172	1.86	1.54
100	0.178	...	2.25	...
50	0.113	...	2.75	...
20	0.038	...	3.21	...

^aCalculated values were obtained by a comparison with this value, which was taken from the literature (Ref. 7).

Thermal diffusivity deduced from data on pyroelectric current produced by pulsed heating from 20 to 290 °K is consistent with data in the literature. Even over this extended temperature range, the mathematical model of Peterson *et al.*,¹ based on considering only the temperature dependence of the thermal diffusivity and the extent of polarization inhomogeneity, is adequate to explain the results.

¹R.L. Peterson, G.W. Day, P.M. Gruzensky, and R.J. Phelan, Jr. *J. Appl. Phys.* **45**, 3296 (1974).

²R.J. Phelan, Jr. and A.R. Cook, *Appl. Opt.* **12**, 2494 (1973).

³G.W. Day, C.A. Hamilton, R.L. Peterson, R.J. Phelan, Jr., and L.O. Mullen, *Appl. Phys. Lett.* **24**, 456 (1974).

⁴G.W. Day, C.A. Hamilton, P.M. Gruzensky, and R.J. Phelan, Jr., *Ferroelectrics* **10**, 99 (1976).

⁵A.I. Baise, H. Lee, B. Oh, R.E. Salomon, and M.M. Labes, *Appl. Phys. Lett.* **26**, 428 (1975).

⁶F.C. Chen, Y.M. Poon, and C.L. Choy, *Polymer* **18**, 129 (1977).

⁷W.K. Lee and C.L. Choy, *J. Polym. Sci. A-2* **13**, 619 (1975).

⁸G. Pfister and M.A. Abkowitz, *J. Appl. Phys.* **45**, 1001 (1974).

⁹K. Takahashi, R.E. Salomon, and M.M. Labes (unpublished).

¹⁰J.B. Enns and R. Simka, *J. Macromol. Sci. B* **13**, 11 (1977).

¹¹E. Fatuzzo and W.J. Merz, in *Ferroelectricity* (North-Holland, Amsterdam, 1967), p. 105.